
Robust Molecular Image Recognition: A Graph Generation Approach

Yujie Qian[†] Zhengkai Tu[‡] Jiang Guo[†] Connor W. Coley[‡] Regina Barzilay[†]

[†]Computer Science and Artificial Intelligence Lab, MIT

[‡]Department of Chemical Engineering, MIT

{yujieq, jiang_guo, regina}@csail.mit.edu {ztu, ccoley}@mit.edu

Abstract

Molecular image recognition is a fundamental task in information extraction from chemistry literature. Previous data-driven models formulate it as an image-to-sequence task, to generate a sequential representation of the molecule (e.g. SMILES string) from its graphical representation. Although they perform adequately on certain benchmarks, these models are not robust in real-world situations, where molecular images differ in style, quality, and chemical patterns. In this paper, we propose a novel graph generation approach that explicitly predicts atoms and bonds, along with their geometric layouts, to construct the molecular graph. We develop data augmentation strategies for molecules and images to increase the robustness of our model against domain shifts. Our model is flexible to incorporate chemistry constraints, and produces more interpretable predictions than SMILES. In experiments on both synthetic and realistic molecular images, our model significantly outperforms previous models, achieving 84–93% accuracy on five benchmarks. We also conduct human evaluation and show that our model reduces the time for a chemist to extract molecular structures from images by roughly 50%.

1 Introduction

In recent years, artificial intelligence has been increasingly utilized for modeling chemistry, in applications such as drug discovery [36, 10, 17, 42] and material design [5, 47]. These models are trained using datasets of chemical reactions, which today are mostly curated by human experts. However, given the rapid growth of scientific discoveries, it is desirable to accelerate this process by automatically extracting such data from the chemistry literature. A distinctive aspect of this extraction task is the recognition of molecular images, which describe chemical structures. In this paper, we aim to parse these molecular images into a machine-readable string format, the Simplified Molecular-Input Line-Entry System (SMILES) [44] string.

While the task of molecular image recognition has been addressed in the past, existing solutions are not robust for practical applications. On one hand, rule-based systems have limited coverage and thus cannot handle input variations [30, 11]. On the other hand, deep learning models perform well on benchmarks but struggle to generalize beyond their training distribution [9, 38, 25]. Generalization is particularly important in this domain as chemistry journals and patents follow a wide range of drawing conventions and liberally utilize abbreviations. At the same time, existing training data are limited and cover only a fraction of possible styles. Therefore, we need to develop a model that can robustly generalize in these conditions.

In this paper, we propose a graph generation approach for molecular image recognition. The basis of our model is an encoder-decoder architecture that encodes the input image into hidden representations and decodes the molecular structure. Different from previous works that directly generate the SMILES string, we predict a *2D molecular graph* that consists of atoms and bonds along with their geometric

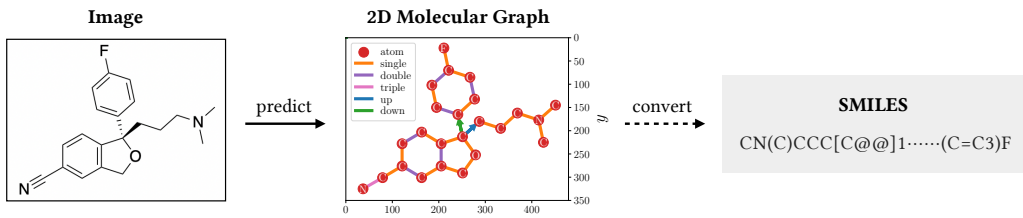


Figure 1: Overview of the graph generation method. We train a model to predict atoms and bonds from the image and construct the molecular graph, then convert into SMILES using chemistry toolkits. The shown example is antidepressant drug escitalopram.

layouts, then convert it into SMILES using chemistry toolkits. Our method naturally extends the image-to-sequence framework by augmenting the output atom sequence with discretized coordinates and adding a separate classifier on top of the decoder to predict the bonds. We further develop data augmentation strategies for both images and molecules as a means of domain randomization [40] to address the domain shift and diverse patterns that may occur in realistic data. Figure 1 gives an overview of the proposed method.

Compared to past work, our model is more flexible in incorporating chemistry constraints. For example, while existing models struggle to correctly determine the chirality of asymmetric carbons, our model conducts geometric reasoning over the predicted graph structure and explicitly applies chemistry rules. Furthermore, the 2D molecular graph formulation is more interpretable due to the atom-level alignment with the image, allowing humans to easily verify the prediction.

We conduct experiments on both synthetic and realistic datasets. In the synthetic experiments, our model outperforms the image-to-SMILES baseline by large margins (3–7%) and shows robust performance on both in-distribution and out-of-distribution test sets. In the realistic experiments, we evaluate the model on four public benchmarks from patents and a new benchmark constructed from publications. Our model achieves 84–93% accuracy, consistently outperforming the baseline and existing systems. Moreover, our model is robust against input perturbation and low-quality images. Finally, we conduct a human evaluation to understand how our model can help chemists to parse molecular images in a semi-automated workflow. The results prove that our graph prediction significantly reduces the time needed by chemists to extract the molecular structure from images. Our model, code, and data are publicly available for future research in molecular image recognition and chemistry information extraction.

2 Related Work

The task of information extraction from scientific literature has been extensively studied, primarily in the natural language processing community [22, 13]. In the chemistry domain, a purely text-based model does not suffice because the text alone does not contain all the necessary information [39, 14]. Molecules are often defined in a figure and referred to by a numerical identifier in the text [2]. Our work focuses on translating the molecular images into a machine-readable format, which is a fundamental component of chemistry information extraction.

Research on molecular image recognition dates back to at least the 1990s and is summarized in a recent survey [31]. Earlier rule-based systems relied on image processing techniques to detect bonds, optical character recognition (OCR) models to detect atom labels, and heuristics to compose the elements into molecular graphs [23, 6, 15, 41, 26, 34, 1, 12]. A few open-source tools have been developed, such as OSRA [11], Imago [37], and MolVec [30]. The usefulness of currently available tools, however, is limited because there are many situations in the literature where designing specific rules is difficult [41]. Rule-based systems are also brittle when the input is perturbed or noisy.

Staker et al. presented a neural network model for molecular image recognition [38]. They formulated the task as image-to-sequence generation, where a convolutional neural network encodes the input image and a recurrent neural network decodes the SMILES sequence. A few variants have been proposed later [32, 33, 9, 18, 45]. These models achieve competitive accuracy on images from the same distribution as their training data, but the performance can degrade severely in real-world scenarios. Besides, they do not provide atom-level alignment with the input, making the prediction

less readable to human. More related to our method, ChemGrapher [25] trained separate classifiers for atoms, bonds, and charges based on image segmentation. This method complicates the recognition task by involving segmentation and relies on pixel-wise labels, which are costly to obtain especially for real-world images. Most recently, Yoo et al. also proposed a graph generation approach for this task, but their decoding algorithm has quadratic time complexity as it re-encodes the graph at each step [46]. Our decoding algorithm is linear and can flexibly enforce chemistry rules. Yoo et al. also predict coordinates as an auxiliary task, while we explicitly utilize them to model stereochemistry. Our approach is simpler and more efficient as we will demonstrate in the experiments.

Our work also relates to the research on learning from synthetic data [29, 16] as synthetic images are used to train our model. To bridge the gap between synthetic and real-world environments, domain randomization methods [35, 40] generate data with more variability by randomizing simulator parameters. We draw inspiration from such techniques and develop data augmentation strategies for molecules and images. Beyond these works, graph generation further improves the robustness.

3 Problem Setup

Molecular image recognition is the task of transforming graphical depictions of molecules into machine-readable chemical structures. Molecules are typically depicted as skeletal formulae (see the example in Figure 1), which consist of atoms and bonds following certain domain-specific conventions [3]. Chemists use chemical structure editors to render molecules, but once the depiction is saved as an image, it is non-trivial for a machine to decode its original structure. Given such an image, the goal is to generate a sequential representation of the molecule, such as the Simplified Molecular-Input Line-Entry System (SMILES) [44] string.

Here, we formulate the molecular image recognition problem. Given an image I of a skeletal formula depiction of molecule mol , our task is to translate it into a SMILES string s that describes its graph structure. We tokenize $s = (s_1, s_2, \dots, s_n)$, where each token either corresponds to an atom or indicates their connections (e.g. parentheses and digits). We define the output as a **2D molecular graph** $G = (A, B)$, where $A = \{a_1, a_2, \dots, a_m\}$ is the set of atoms, $B \subset A \times A \times T$ is the set of bonds, and T is the set of bond types (e.g., single, double, solid wedge, dashed wedge). Each atom a_i is represented by the label¹ ℓ_i and the 2D coordinates of its geometric center (x_i, y_i) .

4 Method

In this section, we propose a novel molecular image recognition model based on graph generation, that is trained on synthetically generated data while remaining robust to real-world molecular images.

4.1 Model Architecture

Our model follows an encoder-decoder architecture. The input image is first encoded into hidden representations with an image encoder. The decoder takes the image encoding as the input and autoregressively generates a sequence of tokens. Previous works [38, 9] directly generate the (tokenized) SMILES string as the output. They mainly have two problems: (1) The generation process is a black box. It is difficult for a human to inspect the predicted SMILES or identify the mistakes; (2) The model struggles to recognize complex chemical patterns, such as stereochemistry, which requires geometric reasoning over the molecular graph.

In this paper, we propose to generate the *2D molecular graph*, i.e. jointly predict the atoms, bonds, and their geometric layout with a unified decoder. Figure 2 demonstrates our model architecture. We use a Swin Transformer [21] as the image encoder and a Transformer decoder [43]. The decoder attends to the image encoding as well as the precedent tokens. Instead of predicting the SMILES string, we construct the molecular graph by explicitly predicting all the atoms (A) and bonds (B) for a given molecular image (I). Formally, the conditional generation process can be written as:

$$P(G | I) = P(A | I)P(B | A, I) \quad (1)$$

where $P(A | I)$ and $P(B | A, I)$ are modeled by an atom predictor and a bond predictor, separately.

¹An atom’s label is its corresponding token in the SMILES, which consists of the chemical element, and optionally its formal charge, isotope, and chirality information.

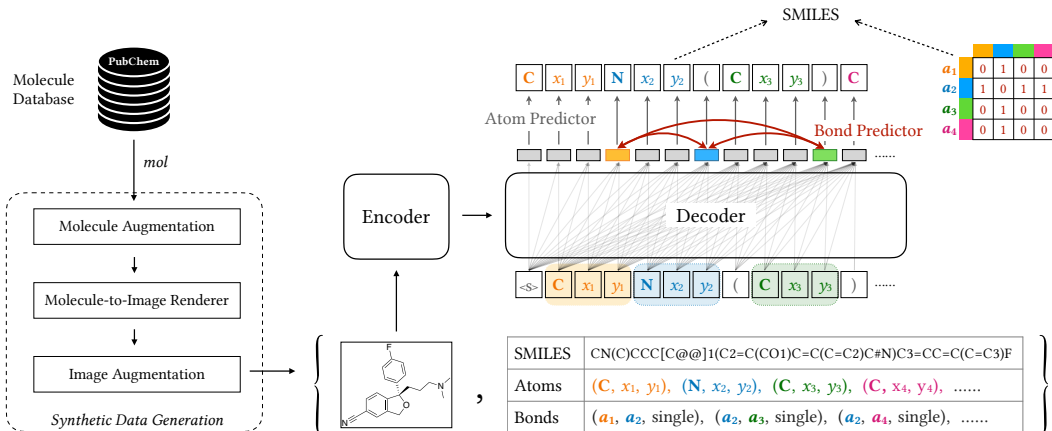


Figure 2: Our model architecture. Molecules are sampled from a database and rendered into images with chemistry toolkits. The model uses an encoder-decoder architecture to generate the 2D molecular graph. The atom predictor outputs the atom labels and their coordinates, and the bond predictor outputs the bonds, which are finally consolidated into SMILES.

The atom predictor is a linear head on top of the decoder’s final layer, which simultaneously predicts atom labels and coordinates. It is inspired by Pix2Seq [7], which formulates object detection as a language modeling task, i.e. generating a sequence of bounding boxes and class labels. In our work, we similarly detect the atoms as objects, but the main difference is that we predict atom coordinates rather than bounding boxes. While the SMILES string contains all the atom labels as tokens, we augment it to include the atoms’ geometric coordinates in the image. Specifically, after each atom token, we insert two tokens representing the atom’s x and y coordinates. The continuous coordinates are converted to discrete tokens by binning. Note that we retain the non-atom tokens in the sequence². Given this construction, the model can autoregressively generate the sequence without additional changes to the architecture. Formally,

$$P(A | I) = \prod_{i=1}^m P(a_i | A_{<i}, I) = \prod_{i=1}^m P(\ell_i | A_{<i}, I) P(x_i | \ell_i, A_{<i}, I) P(y_i | x_i, \ell_i, A_{<i}, I) \quad (2)$$

where each atom a_i is decomposed to three tokens: ℓ_i (label), x_i and y_i (coordinates); $A_{<i}$ stands for the atoms before a_i .

The bond predictor is a feedforward network that operates on each pair of atoms. The decoder converts sequence $[s_1, s_2, \dots, s_{n'}]$ into hidden representations $[h_1, h_2, \dots, h_{n'}]$. For each atom a_i which corresponds to tokens s_k, s_{k+1}, s_{k+2} (label token ℓ_i , coordinates tokens x_i and y_i), we take h_{k+2} as the atom representation. For each atom pair, we concatenate the representations of both atoms as the input to the bond predictor, which classifies the bond type. Formally,

$$P(B | A, I) = \prod_{i=1}^m \prod_{j=1}^m P(\text{bond}(a_i, a_j) | A, I) \quad (3)$$

where $\text{bond}(a_i, a_j)$ represents the bond type between a_j and a_i . An extra “None” type is included to indicate no bond exists between the atom pair.

4.2 Training

The training objective of our model is to maximize the log-likelihood of equation (1). Pairwise training data for realistic molecular images are hard to obtain, as annotating SMILES is time-consuming and requires domain expertise. However, we can take advantage of public molecule databases and

²It is possible to only include the atom tokens, but empirically we observed worse performance when removing the other tokens. As those tokens indicate the connection between atoms, they can help the decoder to model the (sub)graph structure.

chemistry toolkits to construct synthetic training data. In this work, we sample molecules from PubChem [19] and use the Indigo renderer [28] to automatically generate molecular images. We are also able to obtain each atom’s pixel-level (x, y) coordinates in the image through Indigo.

Our preliminary experiments show that the model trained on synthetic data performs poorly on realistic images. There are two major reasons:

1. Real-world molecular images may have chemical patterns that never appear in the synthetically rendered images, such as the usage of abbreviations (e.g. Me, Et, CHO) for functional groups and R-groups (i.e. placeholders for molecule substructures).
2. Different journals publish different standards or templates for drawing molecules, and most chemists have their own styling, thus the realistic images may come from a different distribution than the synthetic data.

To address these challenges, we propose two data augmentation strategies: molecule augmentation and image augmentation.

4.2.1 Molecule Augmentation

The purpose of molecule augmentation is to incorporate the necessary chemistry knowledge about molecular patterns. For example, if the model never sees the pattern “—Me” during training, we cannot expect it to learn the underlying structure of a methyl group (i.e. “—CH₃”). To address this issue, we construct a substitution list of common functional group abbreviations. During training, when a molecule contains a functional group from the list, we randomly replace it according to the substitution rule with a pre-defined probability. The atoms and bonds inside the functional group are removed from the molecule graph, replaced with a “pseudo-atom” with its abbreviation label. We may also randomly add an R-group, whose label is sampled from a list of common R-group labels.

In accordance with our problem formulation, the output SMILES is changed to “pseudo-SMILES” to reflect the functional group replacement and R-group addition. The added “pseudo-atoms” are also associated with labels and 2D coordinates, which are processed in the same fashion as the other atoms. Note that the “pseudo-SMILES” is not a valid SMILES string, but can be converted back to SMILES by expanding the abbreviated functional groups.

4.2.2 Image Augmentation

The molecular images are generated by various software and may have different styles from our synthetic training images, such as text font, bond width and length, and resolution. In order for the learned model to be more robust to different image styles, we develop image augmentation strategies. First, we take advantage of the available rendering options in Indigo to dynamically generate different styles of images for training our model. Second, we apply random data augmentation operations to the image, including rotation, padding, cropping, rescaling, blurring, Gaussian noise, and salt-and-pepper noise. The strategies are designed such that the training images have diverse styles and quality while preserving necessary information of the molecular structures. Details can be found in the appendix.

4.3 Inference

At inference time, we first decode all the atoms and bonds with our model. The molecular graph is constructed based on these predictions. Given the predicted molecular graph, we can flexibly enforce chemistry knowledge and constraints during postprocessing.

We first address the problem of *chirality*, which concerns the relative 3D position of certain atoms that goes beyond connectivity. In images, chirality is described by specific bond types, i.e. solid wedges represent bonds that point out of the plane of the paper, towards the observer, and dashed wedges represent bonds that point into the plane of the paper, away from the observer. In SMILES, however, chirality is specified as an atom property rather than bond type. The symbol “@” after an atom means: looking toward the central atom from the perspective of the first bond, the other bonds are arranged counter-clockwise. In contrast, “@@” after an atom means clockwise. Deep learning models struggle to determine chirality as it requires sophisticated geometric reasoning as well as chemical heuristics. Given the atom coordinates and bond directions surrounding each chiral center, we overwrite its

chirality according to chemistry rules. Note that the 2D atom coordinates are essential here as the chirality cannot be determined from the graph structure alone.

Furthermore, the abbreviated functional group tokens are replaced with their corresponding molecular subgraphs, and the R-group tokens are replaced with wildcards (“*”). This is to be consistent with chemistry conventions, as abbreviations are not allowed in a formal SMILES string.

To ensure the validity of molecule graph, we could add more constraints such as valency checks (e.g., a carbon atom can have 4 bonds at most). However, our model’s default prediction achieves over 99% validity across the test sets, thus additional processing is not necessary. Finally, we derive the SMILES string from the molecule graph using the chemistry toolkit RDKit [20].

5 Experiments

We first validate our method on synthetic data, and then evaluate its performance on images extracted from journal articles and patents. Our code and data are publicly available at https://anonymous.4open.science/r/mol_img_rec/.

5.1 Experimental Setup

Data Our training molecules are randomly sampled from PubChem [19], a public chemical database. We use 200K molecules for experiments, and increase to 1M for training the final model. The images are automatically rendered by chemistry toolkit Indigo [28], with the data augmentation introduced in section 4.2. Molecular graph structure and atom coordinates are also obtained from Indigo. We sample another 5K molecules from PubChem as the validation set. We evaluate our model on both synthetic and realistic benchmarks. Details about the benchmarks can be found in the appendix.

Implementation Details Our image encoder is a pre-trained Swin Transformer³. We resize the input image to the resolution of 384×384 for both training and inference. The decoder is a 6-layer Transformer with 8 attention heads, hidden dimension 256, and sinusoidal positional encoding [43]. Dropout with a probability of 0.1 is applied to the hidden states and attentions. The atom predictor is a linear head on top of the decoder, and the bond predictor is a 2-layer feedforward network with the same hidden dimension as the decoder. All the modules of our model are learned jointly.

During training, we use the maximum learning rate of $4e-4$, linearly warmup for 5% steps, then decay with a cosine function. We use a batch size of 128 and train the model for 50 epochs (25 epochs for training the final model with more data). We apply label smoothing with $\epsilon = 0.1$. The atom coordinates are converted to discrete tokens using 64 bins in both x and y directions (i.e. 6×6 pixels per bin). During inference, we use greedy decoding to generate the output sequence.

Evaluation Metric We evaluate the recognition performance by exact matching accuracy, i.e. the prediction is considered correct if the entire molecular graph structure matches the ground truth. Specifically, we use RDKit [20] to convert both the prediction and ground truth to canonical SMILES, a unique molecule representation, and then compute the string exact match.

Regarding stereochemistry, we add another metric to evaluate the model’s performance on molecules with chiral centers, denoted as chiral accuracy. On the other hand, we ignore the cis–trans isomerism in the evaluation because such information is often not included in the ground truth.

Compared Methods We refer to our proposed method as Graph Generation, and compare it with the baseline SMILES Generation approach. The baseline is trained on the same data and has the same encoder-decoder architecture as our method, as well as all the other training strategies.

In the experiments with realistic images, we also compare with existing molecular image recognition methods, including rule-based systems MolVec [30] and OSRA [11], and a machine learning-based model Img2Mol [9]. Other models, such as MSE-DUDL [38], ChemGrapher [25], and Image2Graph [46], are not publicly available. We show the reported performance in their papers.

³Swin-B (88M parameters), pre-trained on ImageNet-22K. Although molecular images are very different from ImageNet, we found the pre-trained encoder significantly accelerates model learning.

Table 1: Evaluation on synthetic datasets. (scores are accuracy in %; P=PubChem, U=USPTO, I=Indigo, and C=ChemDraw; P+I is an *in-distribution* test set, and the other three are *out-of-distribution* test sets)

	P+I		P+C		U+I		U+C	
	Acc.	Chiral	Acc.	Chiral	Acc.	Chiral	Acc.	Chiral
MolVec	78.72	77.93	78.88	77.72	94.68	92.65	88.13	78.74
OSRA	77.56	77.09	73.18	71.79	94.33	94.38	87.52	78.82
Img2Mol	43.42	–	40.70	–	54.90	–	43.00	–
SMILES Generation	95.41	90.44	81.18	68.25	88.74	74.85	82.53	59.64
- without data augmentation	95.03	89.81	72.56	64.21	86.03	73.64	57.23	30.25
Graph Generation	97.07	94.63	86.04	82.98	95.87	90.49	89.68	78.13
- without data augmentation	95.16	91.77	74.25	72.74	91.40	86.17	72.06	47.97
- continuous coordinates	95.67	92.26	81.17	75.26	89.28	83.49	79.47	70.96
- remove non-atom tokens	96.40	93.68	82.48	82.01	95.28	89.71	89.44	84.36

5.2 Synthetic Data Evaluation

We start with the evaluation on synthetically generated datasets. As our model is trained on molecules sampled from PubChem and synthetic images generated by Indigo, we first construct a test set of 5K molecules from the same distribution. To evaluate the model’s performance on out-of-distribution data, we construct additional test sets from a different molecule and/or image distribution. As a different molecule distribution, we collect a set of molecules from a different source (USPTO). As a different image distribution, we use another software (ChemDraw) to render images. Thus, we have four test sets for synthetic evaluation. As in this experiment the test data are all synthetic, we skip molecule augmentation and apply only image augmentation during training.

The results are shown in Table 1. While the baseline SMILES Generation has achieved over 95% accuracy on the test set from the same distribution (P+I), outperforming rule-based methods by 17%, its performance degrades severely when we test on molecules from a different source or images rendered by different software. When both molecule and image distributions are different (U+C), the baseline performance drops to 58%. Our data augmentation strategy alleviates the distribution shift issue, resulting in an increase of 9–27% accuracy on datasets rendered by ChemDraw.

The proposed Graph Generation approach consistently outperforms SMILES Generation on all four datasets. It achieves a 1.6% accuracy improvement on the in-distribution test set, and 3–7% improvement on out-of-distribution test sets. We observe that a major part of the improvement is credited to our method’s ability to model stereochemistry. SMILES Generation performs poorly on chiral molecules, especially on out-of-distribution datasets, because determining chirality requires geometric reasoning over the 2D graph structure. The SMILES Generation model lacks the ability to do such reasoning. Our method addresses this issue as we explicitly predict the graph.

5.2.1 Ablation Study

We include the ablation results in Table 1. The proposed method predicts atom coordinates as discrete tokens. An alternative approach is to add another head on the decoder to predict continuous coordinates, and jointly optimize it as a regression task. The evaluation results show that the continuous approach performs worse than our discrete approach. We have also tried to remove the non-atom tokens from SMILES in the atom predictor, such as parenthesis, digits, equal signs, but the empirical performance is worse. The non-atom tokens indicate the branching and connection in the SMILES algorithm, thus can help the decoder to better model the graph structure.

We observe that the accuracy of our model drops significantly on large (> 50 atoms) molecules. This is because there are very few large molecules in the training data. However, this issue can be alleviated by upsampling the large molecules. Detailed results can be found in the appendix.

Table 2: Evaluation on realistic datasets. (scores are accuracy in %; † means results from the original paper; – means not available)

	CLEF		UOB	USPTO		Staker		ACS	
	Acc.	Chiral	Acc.	Acc.	Chiral	Acc.	Chiral	Acc.	Chiral
MolVec	77.52	91.67	81.61	88.41	80.73	0.75	0.09	71.57	0.00
OSRA	84.48	93.83	79.30	87.74	78.22	0.02	0.00	80.39	28.57
MSE-DUDL†	–	–	–	–	–	77	–	–	–
Img2Mol	18.55	–	68.69	26.32	–	17.03	–	36.27	–
ChemGrapher†	–	–	70.57	–	–	–	–	–	–
Image2Graph†	51.7	–	82.9	55.1	–	–	–	–	–
SMILES Generation	73.39	54.63	86.53	84.60	51.08	80.78	37.11	75.49	14.29
Graph Generation	80.85	74.69	84.95	90.16	79.26	82.61	49.44	82.35	85.71
- PubChem-only	74.60	74.38	83.14	67.00	57.39	60.77	35.51	72.55	71.43
- USPTO-only	80.24	81.17	6.62	88.00	75.11	81.20	46.93	24.51	14.29
- increase training data	87.50	92.28	86.62	92.90	85.31	83.96	50.27	85.29	98.04

5.3 Realistic Data Evaluation

We also evaluate our model on datasets that are curated from real-world images. We use four publicly available benchmarks, including CLEF, UOB, USPTO [31], and Staker [38]. As these datasets are mostly curated from patents, we collect a new dataset with 102 images from American Chemistry Society (ACS) Publications and manually label their SMILES. We run the existing molecular image recognition systems on these datasets and evaluate them with the same metrics as ours.

Following Staker et al. [38], we collect another training data of (image, molecule) pairs from the United States Patent and Trademark Office (USPTO). This dataset contains more diverse chemical patterns than the synthetic data but is also noisier⁴. We combine the USPTO data with the synthetic PubChem data in section 5.2 to train the models. We start with 200K training examples each from PubChem and USPTO for experiments. As some of the benchmarks are also constructed from USPTO, we filter out those molecules from the training data to ensure no overlap between training and testing.

Table 2 shows the results. Rule-based systems, MolVec and OSRA, perform reasonably well on CLEF, UOB, and USPTO, but almost completely fail on Staker. The images in the Staker dataset are blurry and low resolution, causing rule-based systems to fail. Our model’s performances on all five datasets are significantly better than existing systems. Graph Generation also consistently outperforms SMILES Generation, same as in the synthetic experiment. Img2Mol performs poorly, because (1) Img2Mol is trained only on synthetic data, thus fails to recognize the diverse patterns in realistic images; (2) Img2Mol cannot recognize stereochemistry information (so we omit its chiral accuracy in Table 2). We also show the reported performance of MSE-DUDL [38], ChemGrapher [25], and Image2Graph [46]. Our model achieves much stronger performance, despite trained on much less data (we use 400K examples in total, while MSE-DUDL uses 68M, Img2Mol uses 11M, ChemGrapher uses 1.9M, and Image2Graph uses 7.1M)⁵.

Our model is trained on the combination of PubChem synthetic data and USPTO realistic data. To disentangle the effect of the data, we train models with synthetic or realistic data separately. The PubChem-only (synthetic data) model performs reasonably well but lags behind on patent-based datasets CLEF/USPTO/Staker. The USPTO-only (realistic data) model excels at the patent datasets but performs poorly on other domains, such as UOB and ACS. It shows the two data sources are complementary, thus combining them gives the strongest overall performance. Finally, we increase the amount of training data (1M from PubChem and 1.3M from USPTO) to train our final model. The recognition accuracy further improves on all datasets.

⁴Some of the ground truth from USPTO are incorrect. Besides, only the relative geometric layouts instead of pixel-level exact coordinates are available. We normalize the relative coordinates based on the image size.

⁵Our training data is sampled from the same sources (PubChem and USPTO) as previous works, without any specific data cleaning.

Table 3: Evaluation on perturbed datasets. (scores are accuracy in %)

	CLEF	UOB	USPTO	Staker
MolVec	43.74	74.50	29.74	5.34
OSRA	11.53	68.34	3.99	5.14
Img2Mol	21.12	74.90	29.73	52.60
Ours	84.30	87.16	93.24	68.99

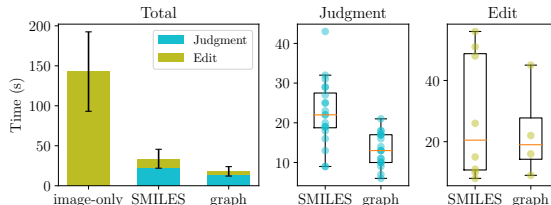


Figure 3: Time for a chemist to convert a molecular image into SMILES, given no additional information, predicted SMILES or graph.

Clevert et al. applied slight perturbations, including rotation and shearing, to the input images, and evaluated their model on the perturbed datasets [9]. We conduct experiments on their released datasets and show the results in Table 3. MolVec and OSRA’s performance drops significantly, although only a small perturbation is applied to the image. Img2Mol performs better, but the performance is still unsatisfactory. Our best-performing model (Graph Generation trained with increased data) achieves much stronger performance on all datasets. It again validates the robustness of our model.

5.4 Human Evaluation

Our graph generation method also has the advantage of being more interpretable. Given the 2D molecular graph predicted by our model, chemists can easily judge if it represents the same molecule as in the image, and correct if there are any mistakes. To verify this point, we invite a student with a bachelor’s degree in chemistry to conduct a qualitative experiment. We randomly sample three groups of molecular image and ask the subject to generate their SMILES strings. As it is difficult to manually write the SMILES string, the subject uses ChemDraw to edit the molecule structure. We compare three different setups: (1) image-only: the subject is given only the image and edits from scratch; (2) SMILES: the subject is given the image and the SMILES predicted by our best model; (3) graph: the subject is given the image and the predicted 2D molecular graph.

In (2) and (3), both the predicted SMILES strings and molecular graphs have been imported into ChemDraw. The subject judges whether the prediction is correct, or edits the predicted structure if there are any mistakes. The difference between (2) and (3) is that when SMILES is imported, the displayed layout often differs from the image, making it harder for the subject to compare. The 2D molecular graph does not have this problem because it is associated with atom coordinates in the given image. The three groups each contains 20 images of similar-sized molecules (34–36 atoms on average). We record the time taken by the subject to make the judgment and edit.

Figure 3 shows the experimental data. In the image-only setup, it takes 143 seconds on average for the chemist to convert an image to SMILES. When the predicted SMILES is provided, the average time reduces to 34 seconds. When the predicted graph is provided, it further reduces to 18 seconds. Breaking down the time for judgment and editing, we find the time reduction is mainly in the judgment part. The results clearly demonstrate the benefits of our graph generation method.

6 Conclusion

In this paper, we propose a graph generation approach for molecular image recognition. Our model is built on an encoder-decoder architecture and jointly predicts atoms and bonds, along with their geometric layout. We design molecule and image augmentation strategies such that the model is robust against the domain shift and diverse patterns in real-world molecular images. Our model is flexible enough to incorporate chemistry constraints such as chirality verification. Evaluations on both synthetic and realistic datasets show strong performance, clearly beating existing rule-based and learned systems. Finally, our model produces more interpretable predictions, allowing chemists to easily verify the structure or correct the mistakes.

We limit the scope of this work to the recognition of single-molecule images. In a complete chemistry information extraction system, we also need models to extract reaction schemes and link figures to texts. Nevertheless, our model achieves robust performance on this subtask.

References

- [1] Maria-Elena Algorri, Marc Zimmermann, Christoph M Friedrich, Santiago Akle, and Martin Hofmann-Apitius. Reconstruction of chemical molecules from images. In *29th Annual International Conference of the IEEE Engineering in Medicine and Biology Society*, pages 4609–4612. IEEE, 2007.
- [2] Edward J Beard and Jacqueline M Cole. Chemschematicresolver: A toolkit to decode 2d chemical diagrams with labels and r-groups into annotated chemical named entities. *Journal of Chemical Information and Modeling*, 60(4):2059–2072, 2020.
- [3] Jonathan Brecher. Graphical representation standards for chemical structure diagrams (iupac recommendations 2008). *Pure and Applied Chemistry*, 80(2):277–410, 2008.
- [4] Alexander Buslaev, Vladimir I Iglovikov, Eugene Khvedchenya, Alex Parinov, Mikhail Druzhinin, and Alexandr A Kalinin. Albuementations: fast and flexible image augmentations. *Information*, 11(2):125, 2020.
- [5] Keith T Butler, Daniel W Davies, Hugh Cartwright, Olexandr Isayev, and Aron Walsh. Machine learning for molecular and materials science. *Nature*, 559(7715):547–555, 2018.
- [6] Richard Casey, Stephen Boyer, Paul Healey, Alex Miller, Bernadette Oudot, and Karl Zilles. Optical recognition of chemical graphics. In *Proceedings of 2nd International Conference on Document Analysis and Recognition (ICDAR’93)*, pages 627–631. IEEE, 1993.
- [7] Ting Chen, Saurabh Saxena, Lala Li, David J Fleet, and Geoffrey Hinton. Pix2seq: A language modeling framework for object detection. *arXiv preprint arXiv:2109.10852*, 2021.
- [8] Bichu Cheng, Johannes Morstein, Lucy Kate Ladefoged, Jannick Bang Maesen, Birgit Schjøtt, Steffen Sinning, and Dirk Trauner. A photoswitchable inhibitor of the human serotonin transporter. *ACS Chemical Neuroscience*, 11(9):1231–1237, 2020.
- [9] Djork-Arné Clevert, Tuan Le, Robin Winter, and Floriane Montanari. Img2mol – accurate smiles recognition from molecular graphical depictions. *Chemical Science*, 12:14174–14181, 2021.
- [10] David K Duvenaud, Dougal Maclaurin, Jorge Iparraguirre, Rafael Bombarell, Timothy Hirzel, Alán Aspuru-Guzik, and Ryan P Adams. Convolutional networks on graphs for learning molecular fingerprints. *Advances in Neural Information Processing Systems*, 28, 2015.
- [11] Igor V Filippov and Marc C Nicklaus. Optical structure recognition software to recover chemical information: Osra, an open source solution, 2009.
- [12] Paolo Frasconi, Francesco Gabbrielli, Marco Lippi, and Simone Marinai. Markov logic networks for optical chemical structure recognition. *Journal of Chemical Information and Modeling*, 54(8):2380–2390, 2014.
- [13] Kata Gábor, Davide Buscaldi, Anne-Kathrin Schumann, Behrang QasemiZadeh, Haifa Zargayouna, and Thierry Charnois. Semeval-2018 task 7: Semantic relation extraction and classification in scientific papers. In *Proceedings of The 12th International Workshop on Semantic Evaluation*, pages 679–688, 2018.
- [14] Jiang Guo, A Santiago Ibanez-Lopez, Hanyu Gao, Victor Quach, Connor W Coley, Klavs F Jensen, and Regina Barzilay. Automated chemical reaction extraction from scientific literature. *Journal of Chemical Information and Modeling*, 2021.
- [15] P Ibison, M Jacquot, F Kam, AG Neville, Richard W Simpson, C Tonnelier, T Venczel, and A Peter Johnson. Chemical literature data extraction: the clide project. *Journal of Chemical Information and Computer Sciences*, 33(3):338–344, 1993.
- [16] Charles Jin and Martin Rinard. Towards context-agnostic learning using synthetic data. *Advances in Neural Information Processing Systems*, 34, 2021.

- [17] Wengong Jin, Regina Barzilay, and Tommi Jaakkola. Junction tree variational autoencoder for molecular graph generation. In *International Conference on Machine Learning*, pages 2323–2332. PMLR, 2018.
- [18] Ivan Khokhlov, Lev Krasnov, Maxim V Fedorov, and Sergey Sosnin. Image2smiles: Transformer-based molecular optical recognition engine. *Chemistry-Methods*, 2(1):e202100069, 2022.
- [19] Sunghwan Kim, Jie Chen, Tiejun Cheng, Asta Gindulyte, Jia He, Siqian He, Qingliang Li, Benjamin A Shoemaker, Paul A Thiessen, Bo Yu, et al. Pubchem in 2021: new data content and improved web interfaces. *Nucleic Acids Research*, 49(D1):D1388–D1395, 2021.
- [20] Greg Landrum. Rdkit: Open-source cheminformatics, 2021. URL <https://www.rdkit.org>.
- [21] Ze Liu, Yutong Lin, Yue Cao, Han Hu, Yixuan Wei, Zheng Zhang, Stephen Lin, and Baining Guo. Swin transformer: Hierarchical vision transformer using shifted windows. In *Proceedings of the IEEE/CVF International Conference on Computer Vision*, pages 10012–10022, 2021.
- [22] Yi Luan, Luheng He, Mari Ostendorf, and Hannaneh Hajishirzi. Multi-task identification of entities, relations, and coreference for scientific knowledge graph construction. In *Proceedings of the 2018 Conference on Empirical Methods in Natural Language Processing*, pages 3219–3232, 2018.
- [23] Joe R McDaniel and Jason R Balmuth. Kekule: Ocr-optical chemical (structure) recognition. *Journal of Chemical Information and Computer Sciences*, 32(4):373–378, 1992.
- [24] Gerry P Moss. Basic terminology of stereochemistry (iupac recommendations 1996). *Pure and applied chemistry*, 68(12):2193–2222, 1996.
- [25] Martijn Oldenhof, Adam Arany, Yves Moreau, and Jaak Simm. Chemgrapher: optical graph recognition of chemical compounds by deep learning. *Journal of Chemical Information and Modeling*, 60(10):4506–4517, 2020.
- [26] Jungkap Park, Gus R Rosania, Kerby A Shedden, Mandee Nguyen, Naesung Lyu, and Kazuhiro Saitou. Automated extraction of chemical structure information from digital raster images. *Chemistry Central Journal*, 3(1):1–16, 2009.
- [27] Adam Paszke, Sam Gross, Francisco Massa, Adam Lerer, James Bradbury, Gregory Chanan, Trevor Killeen, Zeming Lin, Natalia Gimelshein, Luca Antiga, et al. Pytorch: An imperative style, high-performance deep learning library. *Advances in neural information processing systems*, 32, 2019.
- [28] Dmitry Pavlov, Mikhail Rybalkin, Boris Karulin, Mikhail Kozhevnikov, Alexey Savelyev, and A Churinov. Indigo: universal cheminformatics api. *Journal of Cheminformatics*, 3(Suppl 1): P4, 2011.
- [29] Xue Bin Peng, Marcin Andrychowicz, Wojciech Zaremba, and Pieter Abbeel. Sim-to-real transfer of robotic control with dynamics randomization. In *2018 IEEE International Conference on Robotics and Automation (ICRA)*, pages 3803–3810. IEEE, 2018.
- [30] Tyler Peryea, Daniel Katzel, Tongan Zhao, Noel Southall, and Dac-Trung Nguyen. Molvec: Open source library for chemical structure recognition. In *Abstracts of papers of the American Chemical Society*, volume 258, 2019.
- [31] Kohulan Rajan, Henning Otto Brinkhaus, Achim Zielesny, and Christoph Steinbeck. A review of optical chemical structure recognition tools. *Journal of Cheminformatics*, 12(1):1–13, 2020.
- [32] Kohulan Rajan, Achim Zielesny, and Christoph Steinbeck. Decimer: towards deep learning for chemical image recognition. *Journal of Cheminformatics*, 12(1):1–9, 2020.
- [33] Kohulan Rajan, Achim Zielesny, and Christoph Steinbeck. Decimer 1.0: deep learning for chemical image recognition using transformers. *Journal of Cheminformatics*, 13(1):1–16, 2021.

- [34] Nouredin M Sadawi, Alan P Sexton, and Volker Sorge. Chemical structure recognition: a rule-based approach. In *Document Recognition and Retrieval XIX*, volume 8297, page 82970E. International Society for Optics and Photonics, 2012.
- [35] Fereshteh Sadeghi and Sergey Levine. Cad2rl: Real single-image flight without a single real image. *arXiv preprint arXiv:1611.04201*, 2016.
- [36] Marwin HS Segler, Mike Preuss, and Mark P Waller. Planning chemical syntheses with deep neural networks and symbolic ai. *Nature*, 555(7698):604–610, 2018.
- [37] Viktor Smolov, Fedor Zentsev, and Mikhail Rybalkin. Imago: Open-source toolkit for 2d chemical structure image recognition. In *TREC*. Citeseer, 2011.
- [38] Joshua Staker, Kyle Marshall, Robert Abel, and Carolyn M McQuaw. Molecular structure extraction from documents using deep learning. *Journal of Chemical Information and Modeling*, 59(3):1017–1029, 2019.
- [39] Matthew C Swain and Jacqueline M Cole. Chemdataextractor: a toolkit for automated extraction of chemical information from the scientific literature. *Journal of Chemical Information and Modeling*, 56(10):1894–1904, 2016.
- [40] Josh Tobin, Rachel Fong, Alex Ray, Jonas Schneider, Wojciech Zaremba, and Pieter Abbeel. Domain randomization for transferring deep neural networks from simulation to the real world. In *2017 IEEE/RSJ International Conference on Intelligent Robots and Systems (IROS)*, pages 23–30. IEEE, 2017.
- [41] Aniko T Valko and A Peter Johnson. Clide pro: the latest generation of clide, a tool for optical chemical structure recognition. *Journal of Chemical Information and Modeling*, 49(4):780–787, 2009.
- [42] Jessica Vamathevan, Dominic Clark, Paul Czodrowski, Ian Dunham, Edgardo Ferran, George Lee, Bin Li, Anant Madabhushi, Parantu Shah, Michaela Spitzer, et al. Applications of machine learning in drug discovery and development. *Nature Reviews Drug Discovery*, 18(6):463–477, 2019.
- [43] Ashish Vaswani, Noam Shazeer, Niki Parmar, Jakob Uszkoreit, Llion Jones, Aidan N Gomez, Łukasz Kaiser, and Illia Polosukhin. Attention is all you need. In *Advances in Neural Information Processing Systems*, pages 5998–6008, 2017.
- [44] David Weininger. Smiles, a chemical language and information system. 1. introduction to methodology and encoding rules. *Journal of Chemical Information and Computer Sciences*, 28(1):31–36, 1988.
- [45] Hayley Weir, Keiran Thompson, Amelia Woodward, Benjamin Choi, Augustin Braun, and Todd J. Martínez. Chempix: automated recognition of hand-drawn hydrocarbon structures using deep learning. *Chemical Science*, 12:10622–10633, 2021.
- [46] Sanghyun Yoo, Ohyun Kwon, and Hoshik Lee. Image-to-graph transformers for chemical structure recognition. In *2022 IEEE International Conference on Acoustics, Speech and Signal Processing (ICASSP)*, pages 3393–3397. IEEE, 2022.
- [47] Maxim Ziatdinov, Artem Maksov, and Sergei V Kalinin. Learning surface molecular structures via machine vision. *NPJ Computational Materials*, 3(1):1–9, 2017.

A Background

A.1 Graphical Representation of Molecules

Molecules are usually depicted in two dimensions using the **skeletal formula**, following universal conventions [3]. Basic components of the skeletal formula are atoms and bonds. Most common atoms in organic compounds include carbon (C), hydrogen (H), oxygen (O), and nitrogen (N). Two atoms can be connected by a single, double, triple, or aromatic bond. Stereochemistry, i.e. the relative 3D position of certain groups that goes beyond connectivity, can also be denoted in skeletal formulae with special bond depictions [24].

A.2 Sequential Representation of Molecules

Molecules are often represented as sequences for computational convenience. For example, the Simplified Molecular-Input Line-Entry System (SMILES) [44] is a sequential representation of molecule structure in the format of a string, formally defined by a context-free grammar (<http://opensmiles.org/opensmiles.html>).

To generate SMILES, the molecular graph is first turned into a spanning tree by deleting some bonds in the cycles. Numeric suffixes are appended to the two atoms connected by the deleted bond, so that the graph can be reconstructed from the spanning tree. Then SMILES is derived by a pre-order depth-first traversal of the spanning tree, with choices of the starting atom and backbone path. Branching off the backbone is indicated by parentheses. Single bond is usually omitted, while double bond is denoted by “=” and triple bond is denoted by “#”. Figure 4 shows an example to illustrate the SMILES generation algorithm.

Stereochemistry is permitted, but not required, in the SMILES string. First, the chirality of an asymmetric atom is specified by symbols “@” or “@@”. Second, cis-trans isomerism is specified by characters “/” and “\” to show the direction of the single bonds adjacent to a double bond. To determine the stereochemistry requires reasoning over both the molecular graph structure and the geometric positions of atoms.

SMILES is not unique, i.e. a number of equally valid SMILES strings can be written for a molecule. Chemists have developed algorithms to determine the canonical SMILES, which is unique for each molecule. In our work, we allow the model to predict any of the valid SMILES, but convert it to the canonical SMILES during evaluation for easy comparison with the ground truth.

A.3 Chemistry Information Extraction

In chemistry information extraction, a purely text-based model does not suffice because text alone does not contain all the necessary information. Molecules are often defined in the figure and referred to by their numerical identifiers in the textual context. Figure 5 shows an example of extracting

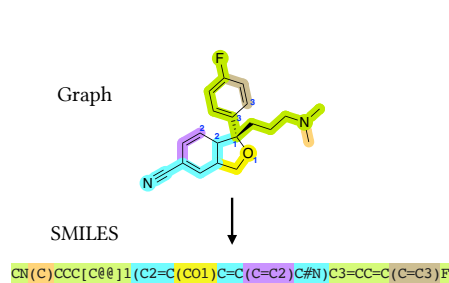


Figure 4: Illustration of the SMILES generation algorithm: cycles are broken and written as branches off a backbone.

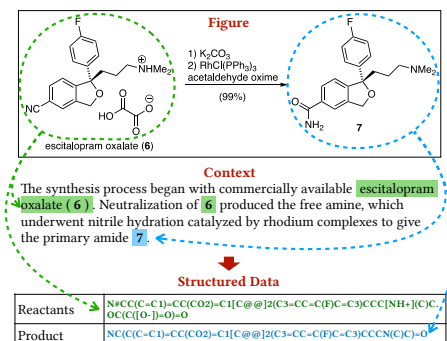


Figure 5: Illustration of chemical reaction extraction from literature. Molecules are presented in the figure and referred to by labels in the context.

Table 4: Summary of test datasets.

Dataset	Source	# image	% chiral
P+I	synthetic	5,000	27.9%
P+C	synthetic	5,000	27.9%
U+I	synthetic	5,719	20.2%
U+C	synthetic	5,719	20.2%
CLEF	patent	992	32.7%
UOB	catalog	5,740	0%
USPTO	patent	5,719	20.2%
Staker	patent	50,000	17.3%
ACS	publication	102	6.9%

chemical reactions from a published paper [8]. An information extraction system needs to transform the molecular images into SMILES strings and jointly reason over the images and texts.

B Experiment Details

B.1 Data

Training The PubChem training data is collected from <https://ftp.ncbi.nlm.nih.gov/pubchem/Compound/>. Unlike previous work, we do not apply any filtering based on molecule size or other properties, but randomly sample the molecules. Images are automatically rendered by the open source toolkit Indigo. We make a few changes to the source code of Indigo to support some rendering options and obtain pixel-level atom coordinates. The changed codes are included in our codebase.

The USPTO training data is downloaded from the same source as [38], the Grant Red Book section of <https://bulkdata.uspto.gov/>. We collect the MOL files and corresponding images. We use RDKit to convert the MOL files to SMILES strings. Relative coordinates, bond types, and special atom labels (functional group abbreviations, R-groups) are parsed from the MOL files.

Test In the synthetic experiment, we construct four test sets with different molecule distributions and image distributions. We sample molecules from PubChem (P) and USPTO (U), and generate images with Indigo (I) and ChemDraw (C).

Our realistic image benchmarks are taken from [31, 38]. CLEF, UOB, and USPTO are downloaded from https://github.com/Kohulan/OCSR_Review, and Staker is downloaded from <https://drive.google.com/drive/folders/160jPwQ7bQ486VhdX4DWpfYzRsTGgJkSu>. The perturbed datasets are constructed by Clevert et al., which are available at <https://github.com/bayer-science-for-a-better-life/Img2Mol/>.

Table 4 summarizes the statistics of the datasets. Figure 6 shows the example images.

B.2 Computational Resource

Our experiments are conducted on a Linux server with 96 CPUs and 500GB RAM. We use four NVIDIA A100 GPUs to train our models. It takes 15 hours to train the base model (with 200K training examples), and about four days to train the final model (with 1.3M training examples). Our implementation is based on PyTorch [27]. The codes and data can be found at https://anonymous.4open.science/r/mol_img_rec/.

B.3 Data Augmentation

Molecule Augmentation Functional groups are often presented as abbreviated labels in molecular images. However, Indigo’s automatic rendering always generates the full structure and never uses abbreviations. We compile a list of 51 common functional group substitution rules, and randomly replace functional groups with their abbreviations in 50% of the training molecules. It is implemented

Dataset	Example Images			
Indigo				
ChemDraw				
CLEF				
UOB				
USPTO				
Staker				
ACS				

Figure 6: Example molecular images in the test sets. The first two rows are synthetic images rendered by Indigo and ChemDraw. CLEF, UOB, USPTO, Staker, and ACS are datasets with realistic images.

by the substructure matching function in Indigo. The full substitution list can be found in our codebase.

We also add R-groups to 50% of training molecules. The R-group label is randomly sampled from the list $[R, R_1, R_2, \dots, R_{12}, R_a, R_b, R_c, R_d, X, Y, Z, A, Ar]$.

Image Augmentation The synthetic training images are dynamically rendered by Indigo with the following options:

- render-background-color: 1,1,1;
- render-relative-thickness: randomly sampled from $[0.5, 1.5]$;
- render-bond-line-width: randomly sampled from $[1, 4]$;
- render-font-family: randomly chosen from {Arial, Times, Courier, Helvetica};
- render-label-mode: randomly chosen from {hetero, terminal-hetero};
- render-implicit-hydrogens-visible: randomly chosen from {true, false}.

We apply image augmentation during training, including the following operations to the image:

- rotate by a random angle from $[-90^\circ, 90^\circ]$;
- crop each side of the image by at most 1%;
- pad one side of the image by at most 40%;
- downscale the image by 15–30% and upscale back;
- blur the image using a random-sized kernel;

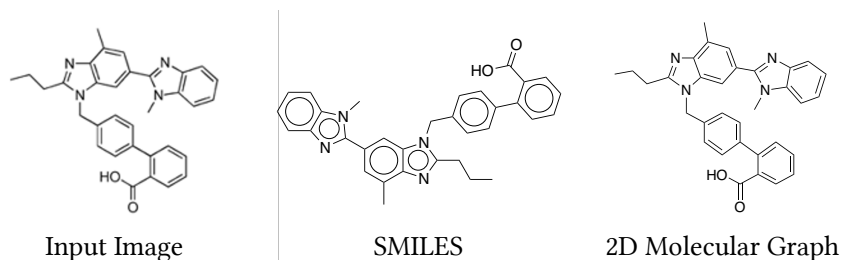


Figure 7: An example in the human evaluation. The middle and right parts correspond to the predicted SMILES and 2D molecular graph, after imported into ChemDraw.

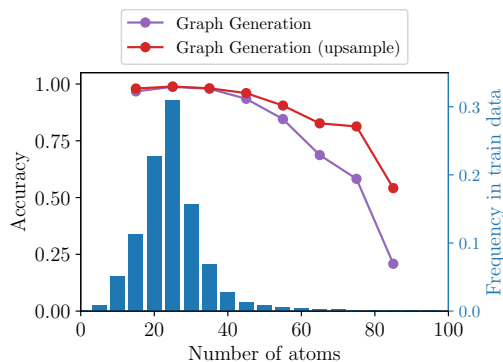


Figure 8: Model accuracy as a function of number of atoms in the molecule. The bars show the training data distribution.

- add Gaussian noise to the image;
- add salt-and-pepper noise (random black pixels) to the image.

Each operation is applied with a probability of 50%. The image augmentations are implemented based on Albumentations [4].

The rendering options and augmentation operations are chosen such that the augmented images have different styles and qualities, and preserve the necessary information for human to generate the molecule structure.

B.4 Human Evaluation

As described in the experiment section, we conduct human evaluation to show how our model can help chemists to parse molecular images. We design three setups, where the subject is given only the image, or associated with predicted SMILES or graph. The predictions are imported into ChemDraw for the subject to edit. Figure 7 presents an example. SMILES does not preserve the coordinates information. Thus after it is imported into ChemDraw, the layout is quite different to the input image, making it circuitous for human to compare. The graph prediction does not have this problem because it is aligned with the image at atom-level.

B.5 Additional Results

We analyze our model’s performance on molecules with different numbers of atoms in Figure 8. The accuracy significantly on large (> 50 atoms) molecules. There are two reasons: (1) recognizing large molecules is harder, as all the atoms and bonds need to be predicted correctly; (2) there are very few large molecules in the training data. We deal with this issue by upsampling the large molecules. When we augment the training data with 100K large molecules, our model’s performance gets significantly improved.